J. Soc. Cosmet. Chem., **27**, 411-431 (September 1976)

Birefringence: Polarization Microscopy as a Quantitative Technique of Human Hair Analysis

ROGER K. CURTIS, B.A. and DON R. TYSON, B.S.*

Presented May 29, 1975, SCC Seminar, St. Louis, Missouri

Synopsis: An alternative to the conventional method of mechanical stress-strain analysis of HUMAN HAIR condition is presented in this paper. NUMERICAL BIREFRINGENCE is an extremely sensitive measure of molecular orientation. As such, this technique has the potential of determining hair fiber condition at a fundamental molecular level. Basic theories of POLARIZATION MICROSCOPY are presented and utilized as the basis of a quantitative technique developed for the measurement of birefringence in hair. The theories, morphological origins, and contributions of both the intrinsic and form birefringence components, and the correlation of numerical birefringence with the mechanical properties of hair are discussed. Numerical birefringence, a quantitative measure of the optical anisotropic properties of a hair fiber cortex, as a reflection of the hair strand condition presently observed with mechanical stress-strain testing, is demonstrated.

Introduction

The traditional method of detemining the condition of a human hair fiber is by measuring its mechanical stress-strain characteristics. The parameters determined, including: Young's modulus; force at yield point; ultimate tensile strength; and either break point extension, or various parameters of elastic recovery hysteresis; (1) are abstract or secondary effects of the basic chemical-molecular occurrences in cosmetic treatment and conditioning. What is needed is an additional system of analysis, which by looking at hair on a foundation molecular level, is more specific.

Crystalline, or molecular chain-sheet substances of a nonisometric nature, exhibit the optical property of birefringence when they are placed in a field of plane polarized light (2). This phenomenon, due to a condition known as

*Redken Laboratories, Inc., Van Nuys, California 91411.

optical anisotropism, is a result of electron orbit polarizability and/or a refractive index differential between a crystal and its surrounding medium in which the crystal is embedded (2, 3, 4). The quantitative measure of birefringence, referred to as the numerical birefringence, is an extremely sensitive measure of optical anisotropism, which arises from molecular orientation (2, 5).

The cortical region of a human hair is optically anisotropic (3, 6). In its function as the major fiber component (7), the cortex contributes 92 per cent to the elasticity of the hair. This is borne out by an analysis of the correlation matrix of a multiple linear regression model that explains the factors contributing to elasticity in hair (8, 14).

In the course of a cosmetic treatment, be it chemical or mechanical in nature, the condition of a hair fiber is changed. The parameter of elasticity, or the resistance to and recovery from deformation by force, plays a major role in the final fiber condition after treatment(1). The change of condition during cosmetic treatment is due to molecular bonding changes, which occur mainly in the cortex (7, 9).

Therefore, the action of cosmetics, which affect condition and elasticity, should also affect the optical anisotropism of the cortex. Thus numerical birefringence, as a very sensitive measure of molecular orientation, emerges as having the potential to very accurately determine hair condition.

This paper presents a quantitative system of analysis of human hair condition, based upon the optical phenomenon of numerical birefringence.

Theory of Birefringe

Plane polarized light is utilized to observe the phenomenon of birefringence. Ordinary light vibrates in waves, traveling in random planes perpendicular to the direction of propagation. By placing a polarization plate in front of a light source, only those waves tarveling in planes parallel to the axis of polarization of the plate are transmitted; the others being absorbed (Fig. 1A).

An anisotropic material has two unique optical properties as follows: (1) any one plane of light waves striking an anisotropic material is split into two wave-planes, traveling 90° relative to each other; and 45° each relative to the original plane of propagation (Fig. 1 B). Hence the term double refraction or birefringence; (2) a plane of light passing through an anisotropic material encounters a path of a different refractive index, and thus travels at a different velocity, in each different direction of traverse (2, 5).

Therefore, a wave of plane polarized light strikes an anisotropic material, is split into two waves, one of which, the ordinary or simply fast wave, is traveling through a path of lesser refractive index, and thus faster than the extraordinary or slow wave, which is traveling at a perpendicular angle in a more difficult path of higher refractive index (2, 5).

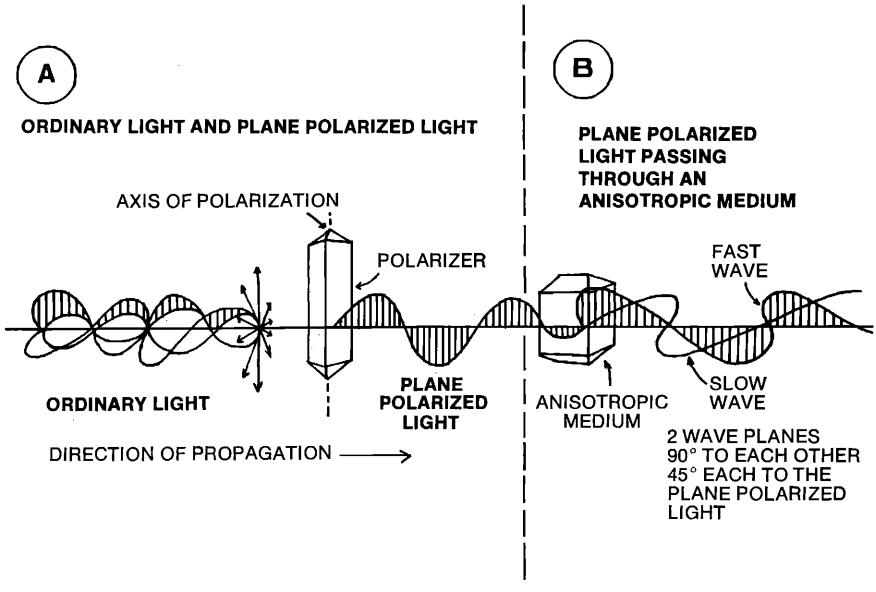

Figure 1. (A) Ordinary light waves being polarized; and (B) ordinary light waves further split into two perpendicular waves, each traveling at different velocity, while traversing anisotropic medium

The difference in refractive index between the two paths of the fast and slow wave (n_2-n_1) equals the numerical birefringence (2).

As the 2 waves advance through the material, the slow wave increasingly lags behind the fast wave in direct proportion to the numerical birefringence (the difference in path velocities) and to the distance or thickness traveled. This quantity of "lag," measured in units of distance, is termed retardation. Hence the formulation, retardation equals numerical birefringence x thickness; or $\Delta = (n_2 - n_1)d$. The numerical birefringence is determined by measuring the retardation and the thickness (2).

The retardation lag of the slow relative to the fast wave causes the two waves to go out of phase with each other (Fig. 2). These two waves, exiting the anisotropic material, interfere with each other, causing an elliptical interference pattern. In Fig. 3(A) the two waves are coming at you in phase with each other, the retardation distance having been some full multiple of the wavelength ($\Delta = n\lambda$). They are vibrating in unison, i.e., each reaching points 1-20 at the same time from points A, A′ to B, B′. The elliptical interference pattern is centered around an axis, formed by connecting the points of intersection of consecutive lines, drawn from the wave position at a particular instant, perpendicular to the wave axis. In Fig. 3(B), the slow wave has been

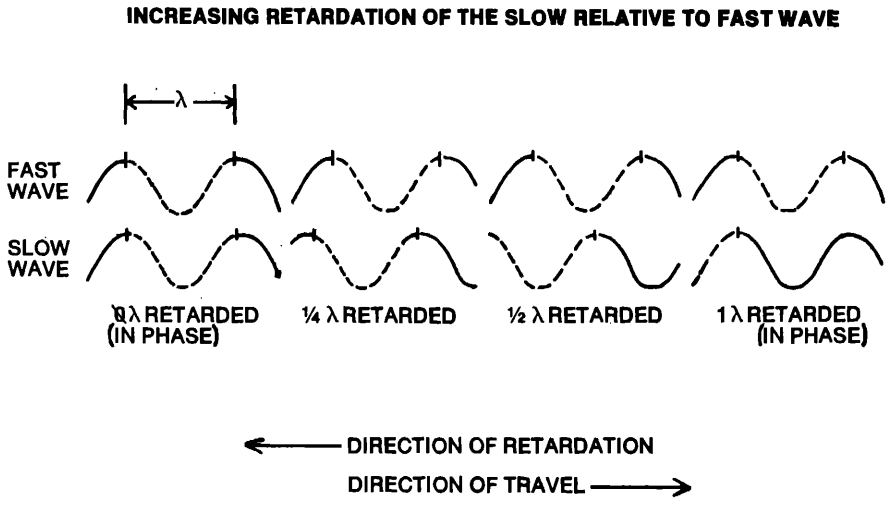

Figure 2. Two parallel waves of equal length λ, traveling at different velocities. As slow wave increasingly retards from fast wave, two go in and out of phase with each other

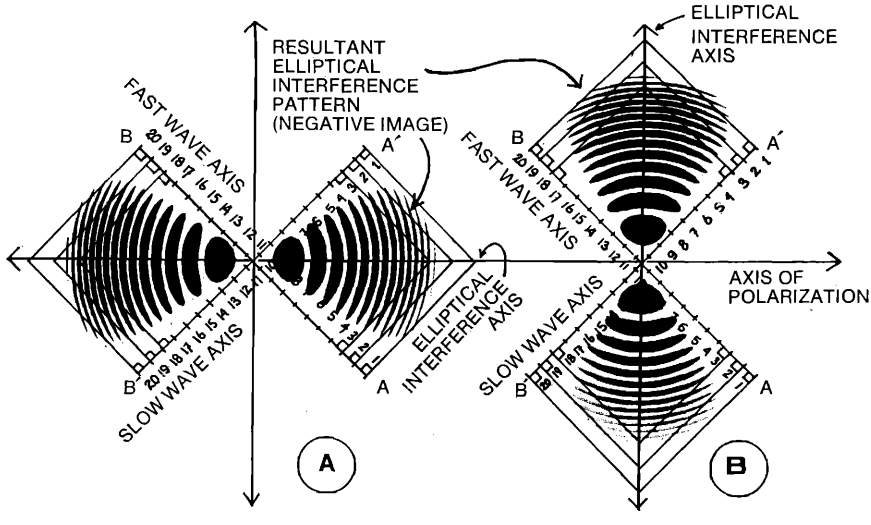

Figure 3. Orientation of elliptical interference pattern formed by two interfering polarized waves; (A) in phase; and (B) ½ λ out of phase (see text)

retarded some full multiple of the wavelength plus one-half ($\Delta = n + \frac{1}{2}\lambda$). In this case, as the fast wave advances from point A, through points 1-20, finally to point B, the slow wave, being ½λ out of phase, advances from point

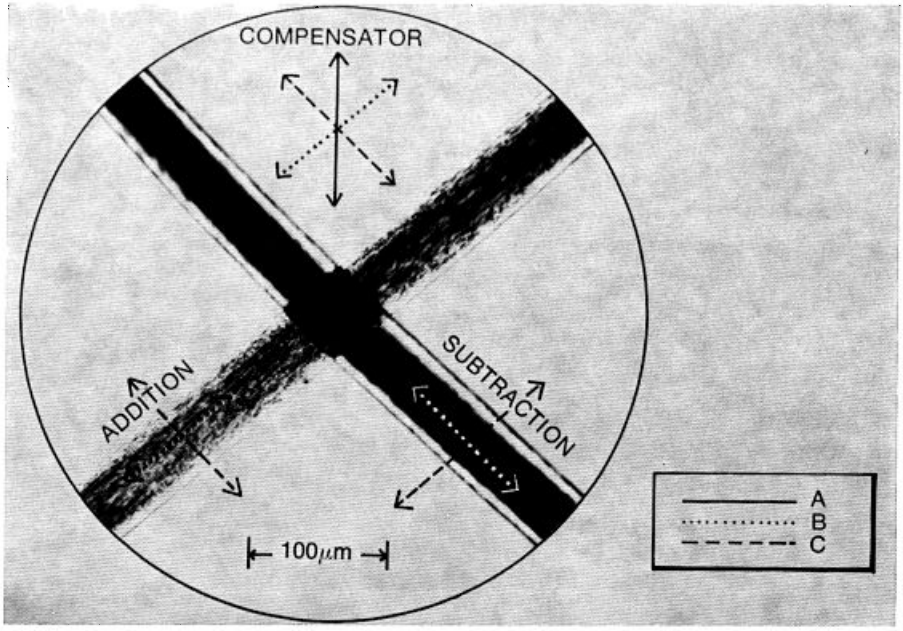

Figure 4. (A) Axis of polarization; (B) slow wave axes of compensator and hair; (C) fast wave axes of compensator and hair. In wave axes of hair and background retardation compensator: parallel alignment produces ***summation*** of their retardations—perpendicular alignment produces ***subtraction*** of their retardations

B′, through points 20-1, finally to point A′; the elliptical interference pattern has shifted 90° (2).

An important concept, utilized in the measurement of numerical birefringence, is that of addition and subtraction of retardation. If anisotropic objects are placed in line (i.e., one on top of another) in the path of light of a polarization system with their slow wave axes parallel, the total amount of retardation in the system equals the sum of the retardation of the individual objects. If, however, the slow wave axes are aligned perpendicular to each other, the total retardation is equal to the difference between the objects as they tend to cancel each other out (Fig. 4) (2).

The anisotropic material being illuminated as has been described (Fig. 1(B)) is viewed through a second polarizing plate, termed the analyzer, whose axis of polarization is 90° to that of the "bottom" polarizer. Only when a portion of the elliptical interference pattern lies in the same axis as that of the analyzer, does light pass; thus, light due to retardation, which in turn is caused by the product of numerical birefringence and thickness, can be seen and measured. No light is passed, a condition referred to as extinction, when $\Delta = n\lambda$; maximum light is passed when $\Delta = n + \frac{1}{2}\lambda$ (Figs. 5 and 6) (2, 5).

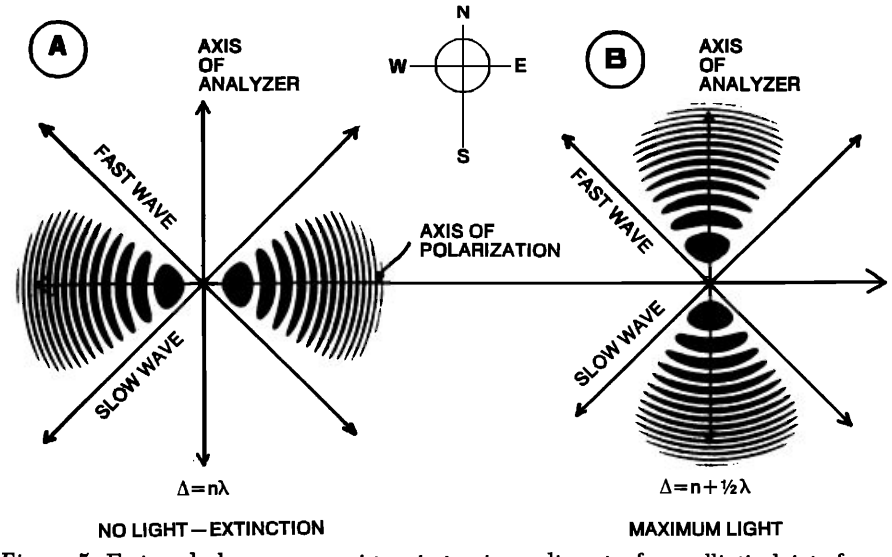

Figure 5. Fast and slow waves exist anisotropic medium to form elliptical interference pattern: (A) $\Delta = n\ \lambda$: the interference pattern is aligned 90° to the analyzer axis; no light can pass; (B) $\Delta = n + \frac{1}{2}\ \lambda$: the pattern is in alignment with analyzer axis; maximum light is transmitted

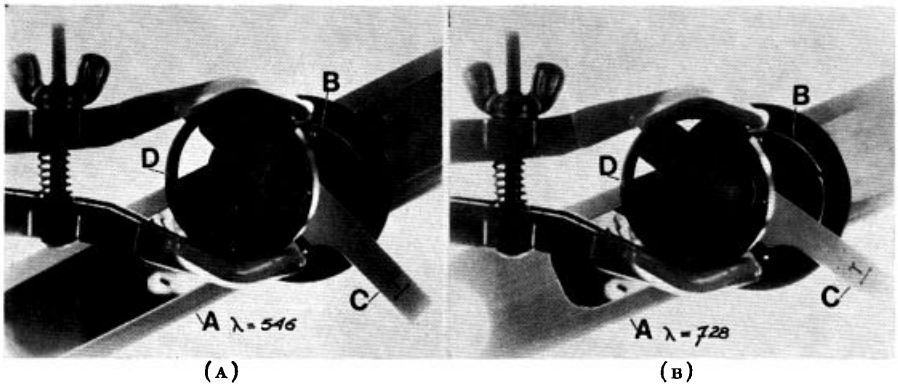

(A) (B)

Figure 6. (A) (A) Light passing through monochrometer of wavelength λ; (B) polarizer; (C) 546 nm retardation compensator; (D) analyzer. (A) compensator causes 1 λ of retardation; no light; (B) [2 compensators (C) are stacked together equaling 1092 nm retardation]. Compensator causes 1½ λ of retardation; maximum light transmission

Until now, only monochromatic light, or light of one particular color and having only one wavelength, has been considered in the theory of birefringence that has been presented. White light is made up of a combination of all wavelengths of light in the visible spectrum, from about 400 to 700 nm. The same phenomena of birefringence and retardation occur, as has been previously described, for monochromatic light with one exception: retardation of a particular distance value will cause some wavelengths or colors of light to be

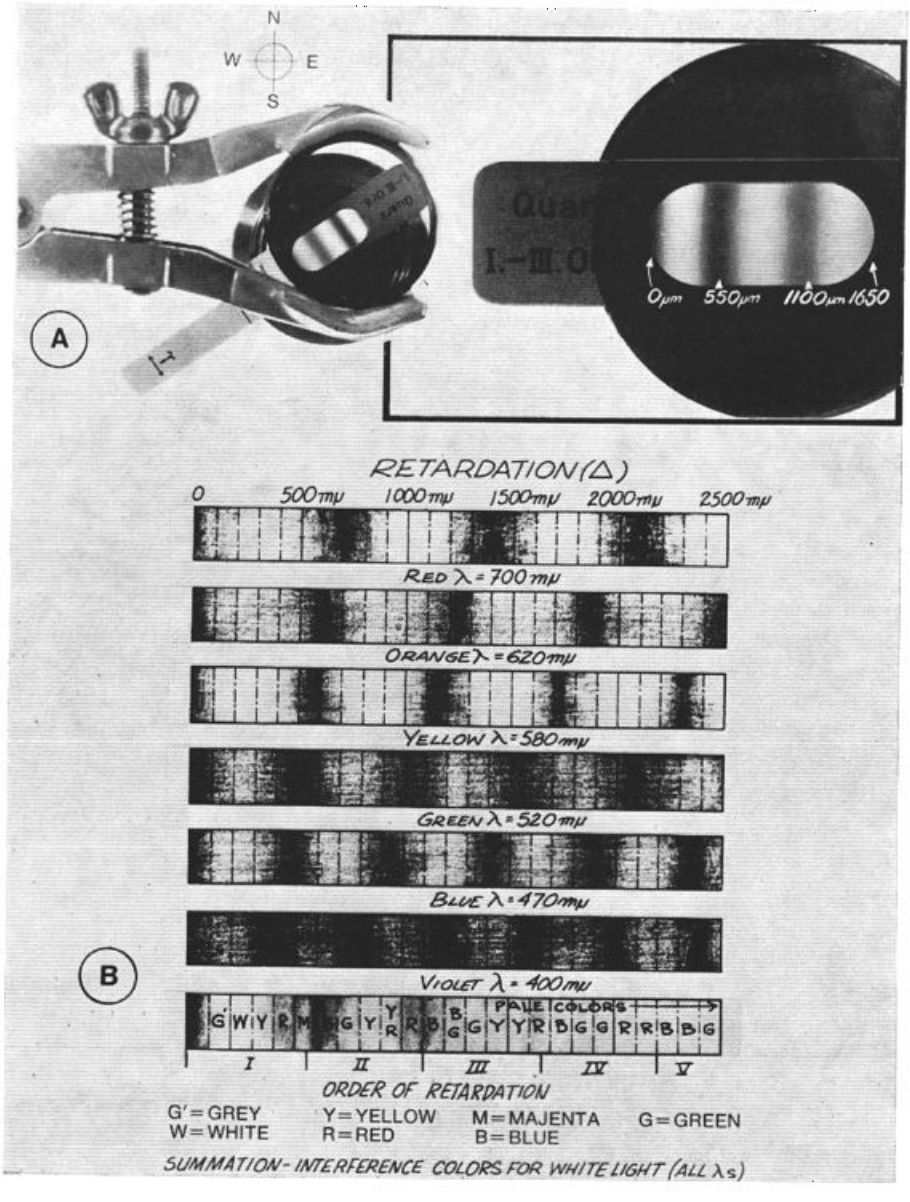

Figure 7. (A) Wedge of aniosotropic quartz causing increasing retardation from 0 μm to 1.650 μm. Note repeating dark bands (representing order of retardation) at intervals of the λ of white light: 550 nm. (B) [Adapted with permission of the publisher (2)], from *Mineral Optics: Principles and Techniques* by Wm. Revell Phillips, W. H. Freeman and Company, copyright © 1971. Retardation of particular value transmitting each color λ differentially. The summation of these λs causes repeating series of colors

in phase, some one-half out of phase, and others out of phase in varying degrees in between. Each of the individual wavelengths will, therefore, pass the top analyzer in a differential amount where they summate, giving a single color or wavelength. Figure 7 is a black-and-white representation of this phenomenon. For a color interpretation of the summation of retardation, refer to Michael Levy's birefringence chart (2).

There are two types of birefringence which occur in an anisotropic material: intrinsic and form (2, 3, 11). Intrinsic birefriengence is a function of the anisotropic polarizability (nonisometric molecular orientation) of electron orbits, and not dependent upon any particular morphology. Form birefringence, however, occurs when crystallites of one refractive index are immersed in a medium of another refractive index. Intrinsic birefringence occurs on a molecular level, whereas form birefringence occurs more on a macromolecular or structural level. The measured quantity, numerical birefringence. is the summation of the intrinsic birefringence and form birefringence (2, 3, 4).

EXPERIMENTAL

Apparatus

Microscope: A Reichert Zetopan research microscope is outfitted for polarization as follows (Fig. 8(A)):

(1) 100 W quartz-iodine lamp house*; (2) strain free, 0.95 N.A., dual-diaphragm condenser;* (3) calibrated-rotating polarizer and analyzer;* (4) 25 X. 0.60 N.A. Neofluar N.A.† objective, checked to be strain free; (5) KPL 8 X Pol Ocular†, modified to contain a measuring reticle; (6) 360° rotating stage*; (7) Gips Rot 1 Ord Compensator* (Fig. 8(B)); and (8) Ehringhaus Compensator with quartz plates† (Fig. 8(B)).

Rotary Device: This device enables a hair fiber to be rotated 360° on its own axis for microscopic viewing and to evaluate structure and measure dimensions (Fig. 8(C)). Two 25x75 mm glass micro slides (i.e., Corning 2948‡). one cut longitudinally with a standard glass cutter, are needed to make 1 reuseable device. The 3 pieces are held together with an epoxy resin glue. It is necessary to use only high quality glass is all parts of the system as any inherent strain present will cause "background" birefringence. A capillary tube ~ 0.5 mm i.d. ~ 1.0 mm o.d., and 75–90 mm long (i.e., Scientific Products B4195-2**), to which a short piece of plastic tubing (Corning Silastic®‡ medical grade tubing 0.035 in. i.d.) is attached, holds the hair for rotation.

The capillary tube is filled with immersion oil. n_D = 1.515, of a light to medium viscosity (Carl Zeiss Immersionsoel†). The holding channel is filled with oil of the same refractive index, but of a higher viscosity to dampen tube movement (i.e., Ziess EinschluBmittel W15†). With a coverslip in place (Corning 22 x 40 mm Number 1-½‡), a nearly homogenous refractive

*Reichert Division of American Optical Scientific Instruments, Buffalo, N.Y. 14215.
†Carl Zeiss, Inc., New York, N.Y. 10018.
‡Corning Glass Works, Scientific Glassware and Equipment Dept., Corning, N.Y. 14830.
**Scientific Products, McGaw Park, Illinois.

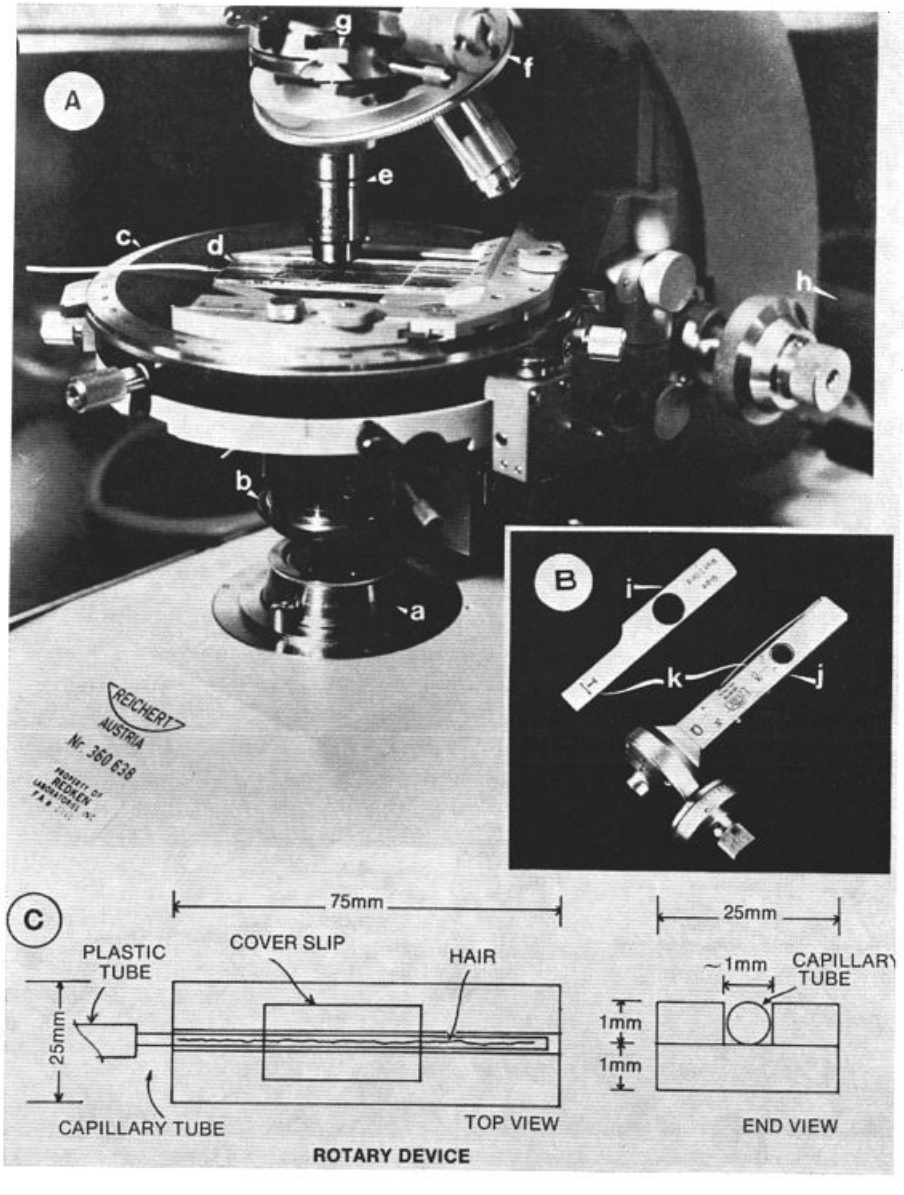

Figure 8. Reichert Zetopan microscope apparatus for determination of numerical birefringence in hair: (A) microscope with (a) polarizer, (b) strain free condenser, (c) rotary stage, (d) rotary device, (e) strain free Neofluar objective, (f) analyzer, (g) compensator, (h) quartz-iodine light source; (B) detail of quartz first order red (i) and Ehringhaus rotary quartz (j) compensators. [Note slow wave axis orientation (k).]; (C) detail of hair rotary device

index path having plane outside surfaces is formed. This arrangement virtually eliminates any distortion, due to the convex surfaces of the capillary tube. Another version of this device has been utilized in previous studies (12).

Stress-Strain Tester

In this study, stress-strain measurements are used as a reference to which the numerical birefringence is compared and correlated. A single hair fiber, 1.9 cm long, is suspended between a set of clamps. Force, applied to one end by a constant speed motor, elongates the fiber at a rate of 1.5 per cent/sec, while being monitored on the other end by a strain gauge transducer.* Stress versus strain graphs are plotted on XY Recorder.†

Procedures

1. *Microscope Alignment;* With the microscopic system having achieved a condition of Kohler illumination, the polarizer and analyzer are inserted and rotated to the correct position. This is best done by first rotating the bottom polarizer to a position of either ϕ, 90, 180, or 270°, and then, while focusing on an illuminated microslide, by rotating the top analyzer until maximum extinction (minimal light transmission) has been reached. If the fixed first-order red compensator plate is now inserted into the compensator slot, a deep red background will appear in the microscope field. This is indicative of a N-S, E-W, polarizer-analyzer alignment, with a diagonal slow-fast wave alignment of the anisotropic compensator (2, 5).

2. *Measurement of Numerical Birefringence in Human Hair Shafts:* To recall, retardation equals numerical birefringence x thickness ($\Delta = (n_2 - n_1)d$). In trying to determine the numerical birefringence, this can be rearranged to read: numerical birefringence equals retardation/thickness ($(n_2 - n_1) = \Delta/d$) (See Fig. 11(B) later on) (2).

A hair shaft of approximately 4 cm length is inserted into the glass capillary tube, into which the medium weight immersion oil is drawn from a reservoir. The capillary can then be plugged and stored in a microhemocrit tube sealer-holder.

*Stathan Instruments, Inc., Oxnard, California 93030.
†Hewlett Packard, Inc., Palo Alto, California 94303.

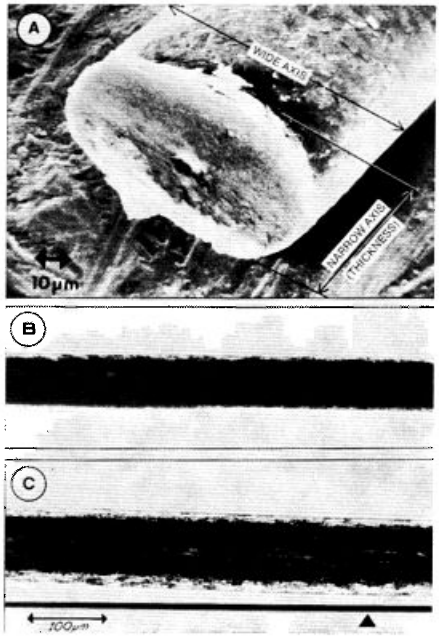

Figure 9. (A) Scanning electron micrograph showing elliptical axes of human hair; (B) hair inside rotary device for measurement on its narrow axis; and (C) on its wide axis. Black line is edge of capillary tube (arrow)

To begin the actual measurement, with the rotary device in place on the microscope stage, a few drops of the heavy weight immersion oil is inserted into the slot, together with the loaded capillary tube, and a coverslip is placed on top. This basic procedure is repeated each time a hair is viewed, as miniature air bubbles, churned by capillary rotation, become trapped under the coverslip, disrupting the homogeneous refractive index, introducing distortion and loss of resolution.

The rotary microscope stage is positioned so that the hair is aligned with its longitudinal axis parallel to the slow wave axis etched on the first order red compensator.

In this position, the slow wave axis of the hair is in the same axis as that of the compensator, giving the hair added retardation providing enhanced viewing ability.

Hair is essentially elliptical in shape, with a wide and narrow axis (Fig. 9(A)). The narrow axis is equivalent to the thickness when the hair is resting on its wide axis, the position used for evaluating the numerical birefringence of the fiber.

The hair is placed exactly on its narrow axis. At that point, both hair edges

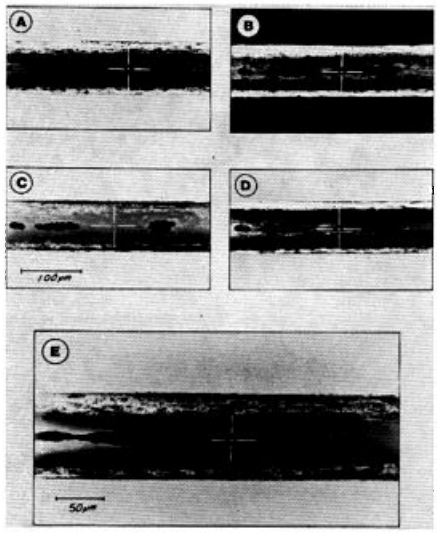

Figure 10. Determination of retardation with Ehringhaus rotary compensator. (Hairs B, C, D, and E are oriented 90° to the compensator.) In series from A through E, colors in hair go down in order i.e., in left to right direction on summation-interference color chart (Fig. 7). (A) hair oriented with quartz first order compensator; (B) Ehringhaus compensator set at ϕ (note extinction background); (C) retardation added to field by compensator with equal amount subtracted from hair; (D) increasing retardation from compensator brings color bands to background and decreased hair center color; (E) all of retardation of hair has been subtracted out in centered black extinction "arrow." From degree of compensator rotation, retardation can be calculated

will appear sharp, the retardation colors will be more or less symmetrically running down the shaft, and the hair will be at its thinnest point (Fig. 9(B)). Record the measurement of the axis with the viewing reticle.

The hair is then rotated 90° where again, the edges will be sharp, the retardation colors symmetrical, and will now be at its widest point (Fig. 9(C)). A measurement of the hair wide axis "diameter" in this position, together with that of the narrow axis, can be put into the formula for the area of an ellipse, 0.5 wide x 0.5 narrow x π, to determine the cross-sectional area. This information is useful in swelling and/or stress-strain analysis.

Next, the retardation must be measured to calculate the numerical birefringence. To do this, the quartz rotary compensator is put in place of the first order red. The hair is to remain on its wide axis, aligned as above. When the rotary compensator is set at ϕ, it is lying flat and has no effect on the system. When it is turned in either direction from ϕ, it adds retardation to the microscopic field by getting effectively thicker to the traversing light. The slow wave axis of the rotary compensator is 90° to that of the first order red (Fig.

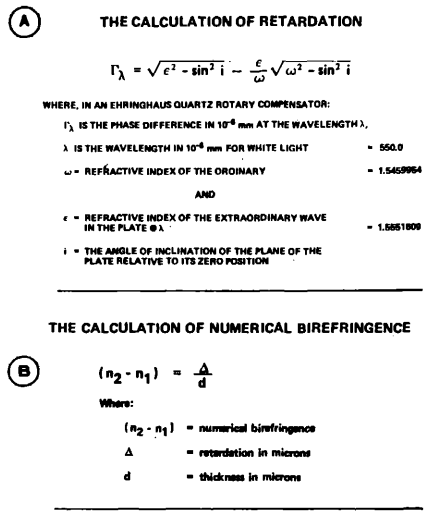

Figure 11.

8(B)). By switching compensators, without changing the orientation of the hair, the slow and fast wave axes of the compensator are now opposed 90° relative to those of the hair, rather than being aligned. Therefore, beginning from ϕ, any retardation added to the microscopic field by rotation of the compensator, is subtracted from the hair. By rotating the compensator, until no birefringence or light is present in the center of the hair or at the edge of the medulla (if present), the retardation can be calculated. Figure 10 portrays this procedure. The compensator reads in degrees of rotation. This has to be converted into microns of retardation through tables supplied with the compensator, or more accurately from a mathematical formula (Fig. 11(A)) (13).

The numerical birefrigence is then determined from the measurements taken (Fig. 11(B)). A programmable microcomputer is used for the various calculations.

The retardation calculation is based upon the use of white light (monochromatic light is not necessary in this system), having a conventional gravity point of $\lambda = 550$, with the Ehringhaus quartz plate compensator fast and slow wave refractive indices being 1.5459954 and 1.5551609, respectively. Precise readings are based upon the assumption that the optical system and the measured object are centered and aligned. In taking readings, the

compensator should be tilted in both directions from ϕ, with their average used in the calculation of retardation. This averaging process tends to cancel out any error caused by eccentricity (13).

Experimentation

Two experiments were conducted to test the significance of numerical birefringence as a measure of hair conditions as follows.

(1) A total of ~ 150 strands from a female Caucasian volunteer with virgin hair were picked at random. Each of these hairs was measured for the following parameters: wide and narrow axis diameter, cross-sectional area, microns of retardation, the numerical birefringence, and stress-strain curve characteristics. Any hairs showing obvious mechanical/chemical damage to the cortex were not used.

A prediction model was set up, utilizing an Olivetti P652 microcomputer* and Olivetti stepwise multiple linear regression program no. 3.03* to look at the contribution of numerical birefringence to the force at yield point (Fig. 12). Utilizing the model, a prediction of the dependent variable, force at 10 per cent elongation, is made from the measured numerical birefringence, the cross-sectional area, and their interaction (the product of the two). The actual prediction is accomplished by putting the three measured values into the solution vector of the model (Table I) (14).

(2) Two hairs, approximately 8 in. long, were cut into 3 parts each and placed in vacuo at $\sim 1 \times 10^{-5}$ Torr overnight. Each of the three parts was picked at random with respect to distance from the scalp, and placed in either 100 per cent glycerol, distilled water, or a solution formulated of the two, to simulate the conditions of 0, 100, and 50 per cent relative humidities (3, 15). Mechanical stress-strain measurements together with diameter and numerical birefringence measurements, were taken within 30 min after immersion into the solution.

Results and Discussion

The results of experiments 1 and 2 are summarized in Table I and Fig. 13, respectively.

An attempt is being made to answer two questions through these experiments as follows: (1) what is the value of numerical birefringence in describing the static condition of a hair fiber; and (2) how does the change of numerical birefringence in a hair fiber relate to the effect of a particular treatment or conditioner? Thus, two proposed uses of numerical birefringence are tested as a measure of human hair condition.

*Olivetti of America, Inc., New York, N.Y. 10022.

MULTIPLE LINEAR REGRESSION MODEL CORRELATING THE OPTICAL/MECHANICAL CHARACTERISTICS OF HUMAN HAIR

$$Y = \beta_0 + \beta_1 X_1 + \beta_2 X_2 + \beta_3 X_1 X_2 + \epsilon$$

WHERE:
- Y = FORCE IN GRAMS @ 10% DEFORMATION
- X_1 = AREA IN SQUARE MICRONS
- X_2 = NUMERICAL BIREFRINGENCE
- $X_1 X_2$ = INTERACTION OF X_1 AND X_2
- ϵ = UNEXPLAINED RANDOM ERROR

$\beta_0 \ldots \beta_3$ ARE THE WEIGHTS THAT ARE ASSOCIATED WITH EACH OF THE MODEL PARAMETERS

Figure 12. Model used to test for contribution and significance of independent parameters

Table I

	1 AREA μm^2	2 NUMERICAL BIREFRINGENCE $(n_2 - n_1)$	3 INTERACTION OF 1 & 2	4 GRAMS FORCE
1		-0.537301	0.896277	0.848987
2			-0.145358	-0.331718
3				0.85443

CORRELATION MATRIX

	$\bar{X}$	σ
1	3743.57	896.57
2	.008763	.000909
3	32.4061	6.1874
4	44.2762	9.2478

PARAMETER DISTRIBUTIONS

SOLUTION VECTOR: N = 143

FORCE (IN GRAMS) = 4.9191 + 0.004361 (area) + 0.7106 (area x numerical birefrigence)

	SE = 0.000952	SE = 0.1380
	t = 4.58	t = 5.084
	df = 140	df = 140
	P < 0.01	P < 0.01

COEFFICIENT OF DETERMINATION = 0.7652

OVERALL F = 228.1795

df = 2,140 P < 0.001

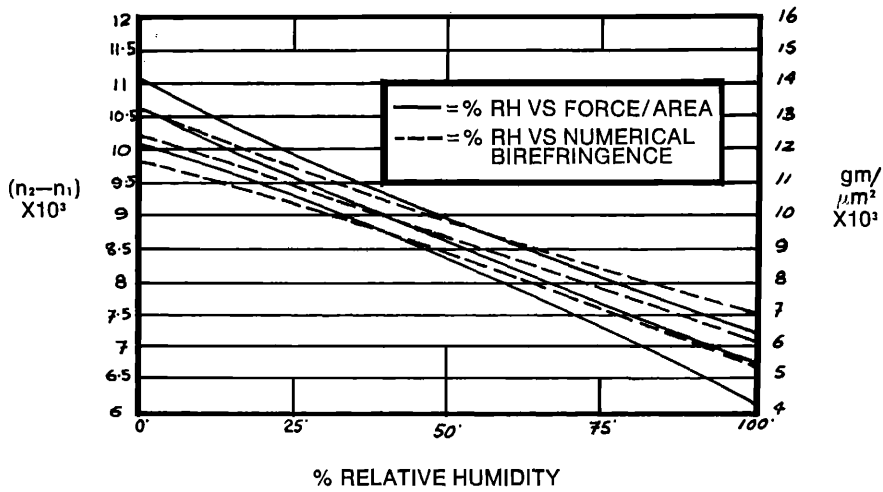

Figure 13. Linear regression with 95 per cent confidence interval of force/area and numerical birefringence versus per cent relative humidity

In the context of this paper, the term condition is used synonymously with the parameter descriptions body and manageability. These, in turn, are more specifically defined as elasticity or the resistance to and recovery from deformation induced by external force. It can be seen by the nature of this definition, that hair condition is traditionally thought of in a mechanical light (1, 9). Obviously, there is a molecular basis to this mechanical behavior (7, 9, 16). The α-helix molecular chain arrangement, basis of the keratin fibril system, is a symmetrically ordered configuration mainly responsible for this longitudinal stability in hair. In addition, both surrounding and infiltrating the fiber system is an amorphous cement-like matrix, which is high in cystine cross-linking, and has both α and β keratin chains (7, 16, 17, 18).

It is this relationship between the fiber system and matrix which becomes important as the contributing factor to both optical and mechanical properties of the hair (3, 7, 9, 16, 17, 18) (Fig. 14).

The mechanical parameters of this relationship can be explained in terms of a two-phase model, which becomes apparent through experimentation with the aqueous swelling of hair (9, 16).

A hair fiber undergoes various changes due to absorbed moisture between the relative humidity levels of 0 to 100 per cent. Approximately 2.7 times less force is required to stress a hair to yield point in a saturated versus dry state. At the same time, swelling occurs at a rate of 16 per cent radially but only

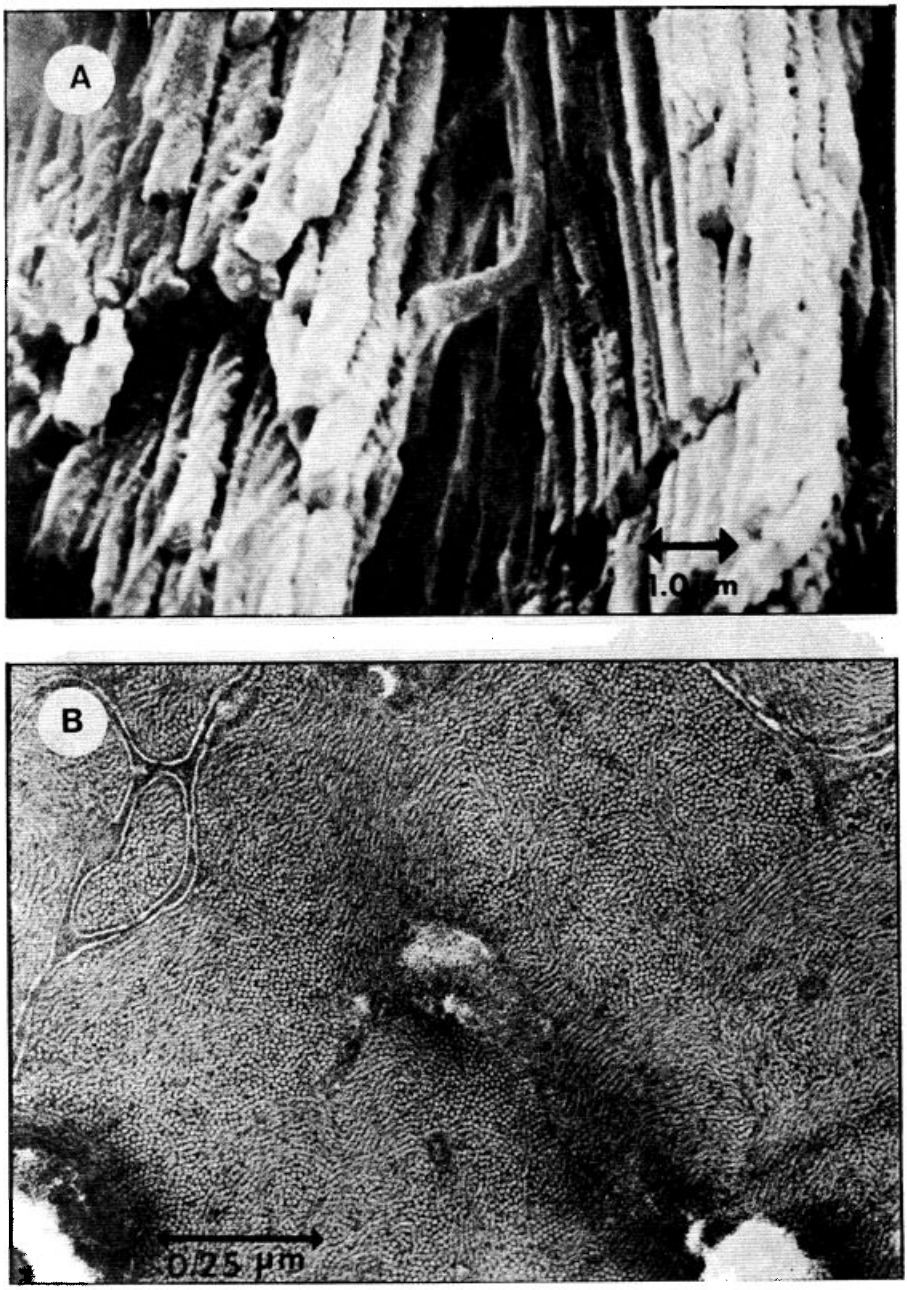

Figure 14. (A) Scanning and (B) transmission electron micrographs of fibril and matrix system in human hair cortex. Note fiber bundles in (A) made up of small fibers, and in (B) the 80 Å protofibrils (small white circles), surrounded by an amorphous matrix (stained dark)

1.2 per cent longitudinally. Equally, there are changes in the torsional-longitudinal modules ratio (9, 16).

The two-phase model is one in which a system of rodlets or fibrils, hydrophobic in nature, are imbedded in an amorphous hydrophilic matrix. Water entering this system affects the hydrogen and salt bonds of the matrix, while the rodlet-fibrils remain relatively unaffected. The swelling experiments bear this out: the rapid rate of radial swelling is indicative of matrix bond breakdown, while the low rate of longitudinal swelling is indicative of the fibril system molecular stability. A reduction in the longitudinal Young's Modulus is indicative of a change in the summation of the fiber matrix relationship, contributing to the total elasticity (3, 7, 9, 16).

These changes are caused by variance in the water content of the fiber as a result of varied relative humidity. Water, in effect, is used as a model conditioning agent for the purpose of these experiments.

Within the realm of cosmetic conditioning and treatment, there also exist more severe agents (i.e., permanent waving solutions and bleaches), which not only affect the hydrogen and salt linkages, as is the case with water, but also the disulphide and even, at the extreme, the fibril backbone peptide bonds. These agents also have an effect equal in magnitude on the two-phase system and ultimately the mechanical-physical properties of hair (1, 7, 20).

This two-phase mechanical model has a rather unique correlation: it emerges surprisingly similar to the classic Frey-Wyssling optical model of composite body-rodlet birefringence (Fig. 15) (19). In this model, rodlet or micellar structures of a crystalline nature are imbedded in a surrounding medium of a different refractive index, as is the case in hair. The rodlet structures themselves are responsible for a contribution to the birefringence of the total system in the mode of intrinsic birefringence. In addition, however, the relationship between the refractive index of the rodlets and their surrounding medium produces form birefringence, which is directly proportional to the difference between the 2 refractive indices of the components. The summation of intrinsic and form birefringence equals the total: numerical birefringence (3, 4, 11 19).

In Table I, the significance of a numerical birefringence system to determine the static condition of a hair strand can be seen. Previous work correlating the molecular orientation of fibrous material, as measured by numerical birefringence, with sonic pulse velocity, which is very well correlated with Young's Modulus in hair, encourages this (21, 22). The correlation matrix explains the contributions of the various parameters to the dependent variable, grams force at 10 per cent deformation, as well as any interactions which occur berween parameters. Cross-sectional area offers the greatest single contribution to the force; a large hair is expected to require more force than a small one. In addition, information about the orientation or integrity of the

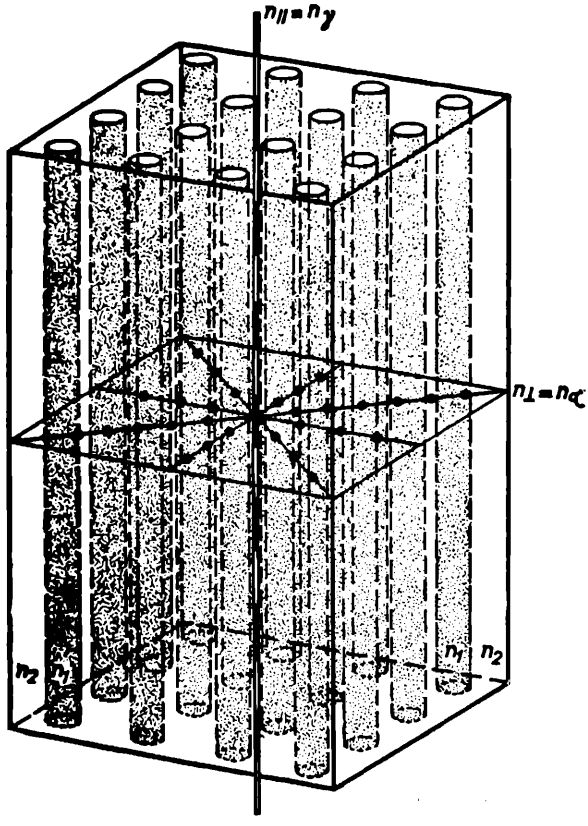

Figure 15. Classical Frey-Wyssling optical model of composite body-rodlet birefringence [with permission of the publisher (19)]

fiber-matrix system can be sought from the numerical birefringence value. This correlation, however, is low and not significant. (It does not appear in the solution vector.) This is due to the inherent characteristics of human hair being such that the numerical birefringence has a tendency to be inversely proportional to the cross-sectional area (the correlation of parameters 2 with 1) and, thus, is not independent. In order to get additional information about orientation and integrity, the interaction term of the cross-sectional area and numerical birefringence must be looked at to correct for nonindependence. This parameter has a correlation of > 0.85 with the grams force.

The solution vector is based upon the 143 hairs placed into the model. It can be seen by the statistical t-values that the 2 parameters, area and the interaction of area and numerical birefringence, are highly significant: $P < 0.01$.

If one takes the 2 measurements from a hair and places them into the solution vector formula, a predicted value of the force in grams at 10 per cent deformation can be obtained. With this model, the coefficient of determination is > 0.76. Thus, more than 76 per cent of the variance of the dependent variable, force in grams, can be explained. This value is significant as is expressed by the high overall F-ratio (228, df 2, 140), and low P-value (<0.001). With the future insertion of additional pertinent variables, as well as a greater sample size base, an additional amount of the unexplained random error can be explained. For more detail about this type of model see (14).

From Fig. 13, it can be seen that both Young's Modulus and numerical birefringence are similarly correlated negatively with relative humidity. A change in relative humidity, or more precisely, a change in water content, inversely changes both the mechanical elasticity and optical anisotropic properties of the hair.

Cosmetic conditioning, or treatments which affect the condition of hair, change the hydrogen and salt bonding arrangements of the matrix, and even the more thermodynamic bonds of the entire cortex, in the case of harsher available cosmetic treatments (7). As a result, there is a change in the mechanical stress-strain characteristic, which is the traditional parameter of measurement, as well as a change in the refractive index of the matrix (1, 3, 7, 9, 16, 20). This causes a change in the form birefringence, in addition to a possible change in the fibrils themselves, causing a change in the intrinsic birefringence (3, 4, 11, 19). Again, numerical birefringence is an extremely sensitive measure of molecular orientation in an anisotropic material (3, 5, 21).

Changes in mechanical elasticity or condition are a result of changes in molecular bonding and orientation (1, 7, 9, 16, 20). In that light, stress-strain analysis appears to be measuring a secondary parameter.

The mechanical method of testing is inherently obtrusive. Required are both an optical device for size determination and a tensile device for mechanical determination. Any inconsistency or flaw over the span of material analyzed tends to bias the results (1).

To build a system of analysis, it is necessary to use certain known parameters of evaluation as a tangible reference to which a correlation can be established. In the case of numerical birefringence, mechanical stress-strain analysis has served this function.

Numerical birefringence is presented as an alternative quantitative system of analysis of human hair condition at the molecular level. With this technique, one is able to determine, unobstrusively, utilizing only one instrument, at specific areas on the shaft, molecular occurrences associated with hair condition and conditioning.

ACKNOWLEDGMENTS

We are deeply indebted to our colleagues of the Biological Research staff for their assistance, especially to Stephen W. Platts for graphic support, and to Dr. David W. Cannell and Dr. Ronald T. Harris for their valuable critique.

(Received October 29, 1975)

REFERENCES

(1) R. Beyak, C. F. Mlyer, and G. S. Kass, Elasticity and tensile properties of human hair. I. Single fiber test method, *J. Soc. Cosm. Chem.*, **20**, 615-26 (1969).
(2) W. R. Phillips, *Mineral Optics—Principles and Techniques*, W. H. Freeman and Company, San Francisco, California, 1971, Pp. 75-101.
(3) A. R. Haly and O. A. Swanepoel, Part V: The nature of birefringence, *Text. Res. J.*, **31**, 966-72 (1961).
(4) H. J. Woods, *Physics of Fibers*, The Institute of Physics, London, 1955, Pp. 50-5.
(5) S. Klosevych, Microscopy and photomicrography, *J. Biol. Photog. Ass.*, **43**, 123-7 (1975).
(6) R. D. B. Frasier, Birefringence and elasticity in keratin fibers, *Nature*, **172**, 675-6 (1953).
(7) A. H. Powitt, Some properties of human hair, presented Australian Society of Cosmetic Chemists Seminar, Terrigal, N.S.W., Australia, April 1967.
(8) Roger K. Curtis and Don R. Tyson, Redken Laboratories, Inc., Van Nuys, CA 91411, unpublished research.
(9) Robert A. Wall and Le Roy D. Hunter, Normal adult hair-structure and properties, *Cosmetics and Perfumery*, **89**, 31-5 (1974).
(10) *Equipment for polarized light microscopy*, Carl Zeiss, Inc., (1972).
(11) R. D. B. Frasier and T. P. MacRae, *Conformations in Fibrous Proteins and Related Synthetic Polypeptides*, Academic Press, New York, 1973, Pp. 159-63.
(12) Vera H. Price, Pseudopili annulati, an unusual variant of normal hair, *Arch Dermatol.*, **102**, 356-7 (1970).
(13) *Rotary Compensator by Ehringhaus, Quartz Plates, Table of Function*, Carl Zeiss Oberkochen/Wurtt, G41-520 d/e/f.
(14) Wm. Mendenhall, *Introduction to Linear Models and the Design and Analysis of Experiments*, Wadsworth Publishing Company, Inc., Belmont, California, 1968, Pp. 1-465.
(15) R. H. Hermans, *Contribution to the Physics of Cellulose Fibres, A Study in Sorption, Density, Refractive Power, and Orientation*, Elsevier Publishing Company, Inc., Amsterdam, 1946, Pp. 21-32.
(16) E. C. Bendit and M. Feughelman, *Encyclopedia of Polymer Science and Technology*, Vol. 8, John Wiley and Sons, Inc., New York, 1968, Pp. 1-44.
(17) R. D. B. Frasier, T. P. MacRae, and G. E. Rogers, Structure of α -keratin, *Nature*, **181**, 592-4 (1959).
(18) Linus Pauling and Robert B. Corey, Compound helical configurations of polypeptide chains: Structure of proteins of the α -keratin type, *Nature*, **171**, 59-61 (1953).
(19) A. Frey-Wyssling, *Submicroscopic Morphology of Protoplasm and its Derivations*, Elsevier Publishing Company, Inc., Amsterdam, 1948, Pp. 57-67.
(20) S. D. Gershon, M. A. Goldberg, and M. M. Rieger, *"Permanent Waving,"* in *Cesmetics: Science and Technology*, Vol. 2, 2nd. ed., M. S. Balsam and E. Sagarin, Ed., Wiley Interscience, New York, 1972, Pp. 174-96.
(21) Henry M. Morgan, Correlation of molecular orientation measurements in fibers by optical birefringence and pulse velocity methods, *Text. Res. J.*, **32**, 866-8 (1962).
(22) Lowell A. Goldsmith and Howard P. Baden, The mechanical properties of hair, *J. Invest. Dermatol.* **55**, 256-9 (1970).